CACR-96-10

An Absorbing-Generating Boundary Condition for Shallow Water Models

A.R. Van Dongeren[1] and I.A. Svendsen,[2] Member, ASCE

ABSTRACT: An absorbing-generating boundary condition based on the Method of Characteristics is derived for the 2D-horizontal nonlinear shallow equations. It allows outgoing waves to leave the computational domain through the boundaries with a minimum of reflection while specifying incoming waves at the same boundaries. The boundary condition's absorbing properties are tested for both linear and nonlinear waves for a range of angles of incidence. Its performance is compared to the classical Sommerfeld radiation condition for the linear case. Also, a case of simultaneous absorption and generation of waves at the same boundary is analyzed.

1 Introduction

When analyzing nearshore problems using numerical models it is usually necessary to limit the computations to a small region around the area of immediate interest. This implies introducing artificial boundaries for the computational region that form the interface to the exterior which is not modelled or is modelled in a simplified way. Thus one of the most important problems in developing time-dependent shallow water models is the specification of accurate boundary conditions

[1]Graduate Student, Center for Applied Coastal Research, Ocean Engineering Lab, University of Delaware, Newark, DE 19716, USA. e-mail: apper@coastal.udel.edu

[2]Professor, Center for Applied Coastal Research, Ocean Engineering Lab, University of Delaware, Newark, DE 19716, USA. e-mail: ias@coastal.udel.edu

along these artificial boundaries because, after long enough time, the performance of these conditions will dominate the model results in the entire computational domain.

These time-dependent models essentially solve approximations to the equations of motion (conservation of mass and momentum) by integration in time of certain dependent variables, typically surface elevation and horizontal velocities. The boundary conditions are required to provide a similar upgrading in time of the same variables along the boundaries.

In developing the nearshore circulation model SHORECIRC (Van Dongeren *et al.*, 1994, 1995), which is capable of describing a number of phenomena (such as edge-waves, surfbeat, longshore currents, shear waves, etc.), we encountered exactly this problem. For our purposes it was necessary to develop boundary conditions on the artificial boundaries that are able to generate a specified long wave and simultaneously absorb outgoing waves, i.e. an absorbing-generating boundary condition.

Most of the existing literature on the topic of artificial boundaries is concerned with absorbing (sometimes called *radiating*, *non-reflective* or *open*) boundary conditions specifically derived for the wave equation or the shallow water equations. For a thorough review on this subject, we refer to Givoli (1991).

In one of the most frequently quoted papers, Engquist & Majda (1977) [E&M] developed a perfectly absorbing boundary condition which is nonlocal in space and time. This means that the complete time history along the entire boundary is required in order to update the variables at any point along the boundary in time. Because this is very impractical for any numerical application, E&M derived local approximations to the general solution of increasing order of accuracy. The approximations are centered around chosen angles of incidence θ_n between the boundary

normal and the direction of the outgoing waves. Higdon (1986, 1987) derived a general form of this radiation condition and showed that it can be written as

$$\left(\frac{\partial}{\partial t} + \frac{c_o}{\cos\theta_n}\frac{\partial}{\partial x}\right)^n u = 0 \tag{1}$$

where n is the order of accuracy and c_o is the linear phase speed. This expression gives the best absorption when the angle of the outgoing wave to the normal is θ_n. For $\theta_n = 0^o$ the equation reduces to E&M's boundary condition, which only absorbs normally incident waves optimally. To the first order of the approximation ($n = 1$), the E&M boundary condition further reduces to the Sommerfeld radiation condition (Sommerfeld, 1964)

$$\left(\frac{\partial}{\partial t} + c_o\frac{\partial}{\partial x}\right) u = 0 \tag{2}$$

which essentially states that the outgoing wave is propagating in the positive direction without change of form. Eq. (1) was also found independently by Keys (1985) and is an improvement over the boundary condition developed by E&M because the reflection coefficient can be greatly reduced if the angle of incidence θ_n is known in advance. This might be the case for some types of problems (e.g., waves radiating from a source inside the computational domain), but not for the more general models we are considering here.

Another disadvantage of this type of boundary condition is that the solution to the problem is assumed to have a certain form. Broeze & Van Daalen (1992) did not make that assumption and derived a boundary condition from the local energy flux in the normal direction to the boundary using the variational principle and showed improved accuracy when used in a panel method.

Unfortunately, the above mentioned boundary conditions are only capable of absorbing waves and (except for Broeze & Van Daalen) only address the linear problem. Hibberd (1977) considered the more general problem of simultaneously

generating and absorbing waves and derived a boundary condition for the nonlinear shallow water equations (NSW) where the outgoing wave is calculated using the Method of Characteristics while an incoming Riemann variable associated with an incident uniform bore is specified. On a similar basis Verboom *et al.* (1981) gave more general expressions for weakly-reflective boundary conditions based on the specification of incoming Riemann variables. Verboom & Slob (1984) derived two orders of approximation of this type of boundary condition and calculated reflection coefficients which were of the order of a few percent. However, the applications in both papers only deal with situations where no incoming wave is specified and the boundary condition reduces to the case of absorption only.

In the case of simultaneous absorption and reflection, it is not possible to specify the incoming Riemann variable since it is a function of the unknown surface elevation and velocity. Instead, Kobayashi *et al.* (1987) used the outgoing characteristic and substituted a linear long wave relationship between the velocity and the surface elevation to solve for the outgoing wave. They only solve the problem for one horizontal dimension, equivalent to the case of normal incidence and did not report on the accuracy of the boundary condition. The present paper gives an extension of Kobayashi *et al.* (1987)'s boundary condition to the general case of two dimensions and expands the condition to a higher order of approximation.

The outline of this paper is as follows. In Section 2 we discuss the formulation of the problem. In Section 3 the boundary condition is derived from the fundamental equations for two orders of the approximation. In Section 4 the reflection properties of both versions are investigated for the case of absorption only and compared to the classical Sommerfeld radiation condition for the linear case. In Section 5 the boundary condition is further tested for the case of simultaneous generation and

absorption at the same boundary.

2 Formulation of the problem

The boundary conditions we specify along the artificial ocean-side boundaries must guarantee a unique and well-posed solution to the differential equations. As may also be inferred from the literature review given above, this is not a straightforward problem, and it appears that to some extent waves and currents need to be addressed separately.

From the outset one would expect that the idea of emulating the effects of a large ocean in a computation that only covers a small region of that ocean imposes some limitations on what can actually be represented in the model, and this is true. More importantly, however, it also requires a clarification of which physical mechanisms we should actually try to describe along those boundaries.

Our requirements can be formulated by stating that the boundary conditions need to satisfy two criteria:

1. The region outside the computational domain can only influence the motion inside through the incident (long) waves and through the currents along the boundaries. Thus we must assume that we know and can specify those currents and incident waves.

2. (Long) waves propagating out of the computational region must be allowed to propagate freely through the open ocean-side boundaries with minimal reflection.

It turns out that whereas outgoing waves can be separated from the total signal and absorbed at the artificial boundaries, this is not the case for currents. The distribution of the currents is essentially an elliptic problem and therefore the currents have to be specified along the entire boundary to uniquely specify the problem. This also implies, however, that in the general case extensive information is needed about the currents outside the domain in order to be able to specify the currents along the computational boundary.

Finally it raises the question of how to distinguish between waves and time-varying currents. A closer inspection of this problem suggests that this is a matter of the time scale of the variations relative to the time it takes for a disturbance to propagate across the computational domain. For simplicity, we limit our scope in the present paper to the case of incident long waves without currents.

Thus the boundary conditions must be able to generate a specified long wave and simultaneously absorb outgoing waves, in the presence of known currents and ideally without much additional computational effort.

3 Derivation of the boundary condition

The governing equations of the SHORECIRC model are the depth-integrated, shortwave averaged continuity and momentum equations (Van Dongeren *et al.*, 1994; Svendsen & Putrevu, 1995). If we place the open boundaries carefully we can achieve that near these boundaries the local forcing is weak. This means that the dominating terms in the continuity and momentum equations are the terms corresponding to the nonlinear shallow water (NSW) equations in matrix form:

$$\frac{\partial}{\partial t}\begin{bmatrix}\bar{u}\\ \bar{v}\\ h\end{bmatrix}+\begin{bmatrix}\bar{u} & 0 & g\\ 0 & \bar{u} & 0\\ h & 0 & \bar{u}\end{bmatrix}\frac{\partial}{\partial x}\begin{bmatrix}\bar{u}\\ \bar{v}\\ h\end{bmatrix}+\begin{bmatrix}\bar{v} & 0 & 0\\ 0 & \bar{v} & g\\ 0 & h & \bar{v}\end{bmatrix}\frac{\partial}{\partial y}\begin{bmatrix}\bar{u}\\ \bar{v}\\ h\end{bmatrix}=\begin{bmatrix}g\frac{\partial h_o}{\partial x}+f_x\\ g\frac{\partial h_o}{\partial y}+f_y\\ 0\end{bmatrix} \quad (3)$$

where h is the total water depth $h = h_o + \bar{\zeta}$, h_o is the still water depth and $\bar{\zeta}$ is the shortwave averaged surface elevation. $\bar{u}$ and $\bar{v}$ are the depth averaged and shortwave averaged velocities in the x and y directions, respectively. See Fig. 1 for a definition sketch. It may be worth emphasizing that since we are considering the general case of short wave motion with arbitrary time variation, the shortwave averaged $\bar{\zeta}$ and $\bar{u}, \bar{v}$ represent surface elevation and particle motion, respectively, in the infragravity wave motion. Usually $\bar{\zeta}$ will also include a steady set-down or set-up component. f represents all the local forcing terms for the motion, which comprise the radiation stress gradients, the current-current and current-wave integrals (originating from the non-uniform variation of the velocities over depth) and the bottom and wind shear stresses. These effects are all included in the original equations.

Following the procedure outlined in Whitham (1974) and Abbott (1979), the eigenvalues and eigenvectors are obtained from this system of equations. The three eigenvectors span the space P:

$$P = \begin{pmatrix} \cos\vartheta & \cos\vartheta & \sin\vartheta \\ \sin\vartheta & \sin\vartheta & -\cos\vartheta \\ \sqrt{\frac{h}{g}} & -\sqrt{\frac{h}{g}} & 0 \end{pmatrix} \quad (4)$$

where ϑ is the angle between the normal to the boundary and the x-axis as identified by Verboom *et al.* (1981) (see Fig.2). Premultiplying the system of equations (3) with P^{-1} yields the governing equations in characteristic form as derived by Verboom *et al.* (1981). (Please note that the eigenvectors in their Eq. (11.5) contain a typo and are therefore not identical to the matrix P.)

It is convenient to choose the x-axis normal to the seaward boundary of our rectangular domain, which sets $\vartheta = 0$. The equations in characteristic form then simplify to:

$$\frac{\partial \beta^-}{\partial t} = -(\bar{u} - c)\frac{\partial \beta^-}{\partial x} - \bar{v}\frac{\partial \beta^-}{\partial y} + c\frac{\partial \bar{v}}{\partial y} + g\frac{\partial h_o}{\partial x} + F_{\beta-} \tag{5}$$

$$\frac{\partial \beta^+}{\partial t} = -(\bar{u} + c)\frac{\partial \beta^+}{\partial x} - \bar{v}\frac{\partial \beta^+}{\partial y} - c\frac{\partial \bar{v}}{\partial y} + g\frac{\partial h_o}{\partial x} + F_{\beta+} \tag{6}$$

$$\frac{\partial \gamma}{\partial t} = -\bar{u}\frac{\partial \gamma}{\partial x} - \bar{v}\frac{\partial \gamma}{\partial y} - g\frac{\partial \bar{\zeta}}{\partial y} + F_\gamma \tag{7}$$

In (5) the Riemann-invariant β^- is defined as

$$\beta^- = \bar{u} - 2\,c = \frac{Q_x}{(h_o + \bar{\zeta})} - 2\sqrt{g\,(h_o + \bar{\zeta})} \tag{8}$$

where Q_x is the total flux in the x direction and $\bar{u}$ is the depth averaged velocity. The Riemann-invariant of (6) is similarly defined as $\beta^+ = \bar{u} + 2c$. It turns out that the γ-equation is the y-momentum equation itself which has the Riemann-invariant

$$\gamma = \bar{v} = \frac{Q_y}{(h_o + \bar{\zeta})} \tag{9}$$

The definition sketch in Fig. 3 shows that β^+ propagates along a characteristic in the positive x direction, β^- in the negative x direction and γ in the y direction. The forcing terms $F_{\beta+}$, $F_{\beta-}$ and F_γ originate from the f-terms in (3). These terms imply that β^+, β^- and γ vary along their characteristics and the invariants should therefore actually be called Riemann *variables*.

During the computation we will at time step n know the total value of $\bar{\zeta}^n$ and (Q_x^n, Q_y^n) at interior as well as boundary points. The incoming wave motion is specified along the $x = 0$ boundary through specification of $(Q_{x,i}, Q_{y,i})$. The governing

equations (3) will then provide the values of the total $\bar{\zeta}, Q_x, Q_y$ for interior points in the domain, and the problem is to determine the equivalent total values along the boundary at time step $n+1$. In this process we also determine the parameters of the outgoing wave.

In the following, the absorbing-generating boundary condition for two different orders of the expansion are derived for a boundary along the y-axis ($x = 0$) only. The results can readily be generalized to arbitrary boundary directions which is omitted here.

Assuming linear superposition of the incoming wave (subscripted i in the following) and the outgoing wave (subscripted r) we can write

$$Q = Q_{x,i} + Q_{x,r} \qquad \bar{\zeta} = \bar{\zeta}_i + \bar{\zeta}_r \tag{10}$$

Without further approximation the incoming Riemann-variable (8) can then be rewritten as

$$\begin{aligned} \frac{\beta^-}{c_o} &= \frac{Q_{x,i}}{c_o h_o}\left(1 + \frac{\bar{\zeta}_i + \bar{\zeta}_r}{h_o}\right)^{-1} + \frac{Q_{x,r}}{c_o h_o}\left(1 + \frac{\bar{\zeta}_i + \bar{\zeta}_r}{h_o}\right)^{-1} \\ &- 2\sqrt{1 + \frac{\bar{\zeta}_i + \bar{\zeta}_r}{h_o}} \end{aligned} \tag{11}$$

where

$$c_o = \sqrt{g h_o} \tag{12}$$

At this point we introduce the assumption that the total volume flux in the direction of the wave propagation is related to the surface elevation by the equation:

$$Q = c(\bar{\zeta} - \bar{\bar{\zeta}}) + \bar{Q} \tag{13}$$

where $c\,\bar{\zeta}$ represents the volume flux in the oscillatory part of the motion. $\bar{Q}$ is the net volume flux which consists of the nonlinear mass flux, Q_w, in the infragravity

waves and the "current". $\bar{\bar{\zeta}}$ is the average over the infragravity wave period of the infragravity wave surface elevation $\bar{\zeta}$. It has been shown (see e.g. Svendsen (1974) or Svendsen & Justesen (1984) for two different derivations) that this relationship, which is purely kinematical, is exact for plane waves of constant form, no matter what height or nature. Thus the use of this relationship here only implies that assumption for the incoming and outgoing wave motion in the neighborhood of the boundary in question. (Svendsen & Justesen (1984) found that even for waves deforming rapidly towards breaking, the error from using this relationship was less than 5%).

For simplicity we assume in the following that $\bar{\bar{\zeta}}$ as well as $\bar{Q}$ are zero. Then, again using linear superposition, Eq. (13) for the x-component of Q_i and Q_r can be written as

$$Q_{x,i} = c\,\bar{\zeta}_i \cos\theta_i \qquad Q_{x,r} = -c\,\bar{\zeta}_r \cos\theta_r \tag{14}$$

where θ_i and θ_r are defined as the angles between the normal to the boundary and the incoming and outgoing waves in the range $[-\frac{\pi}{2}, \frac{\pi}{2}]$, respectively. Eq. (11) then becomes

$$\begin{aligned}\frac{\beta^-}{c_o} &= \frac{Q_{x,i}}{c_o h_o}\left(1 + \frac{Q_{x,i}}{h_o c\cos\theta_i} - \frac{Q_{x,r}}{h_o c\cos\theta_r}\right)^{-1} + \frac{Q_{x,r}}{c_o h_o}\left(1 + \frac{Q_{x,i}}{h_o c\cos\theta_i} - \frac{Q_{x,r}}{h_o c\cos\theta_r}\right)^{-1} \\ &- 2\left(1 + \frac{Q_{x,i}}{h_o c\cos\theta_i} - \frac{Q_{x,r}}{h_o c\cos\theta_r}\right)^{\frac{1}{2}}\end{aligned} \tag{15}$$

Here we can expect that $Q_x/h_o c_o \ll 1$. If we expand this expression to first order with respect to $Q_x/h_o c_o$ and solve with respect to $Q_{x,r}$ we get

$$Q_{x,r} = \frac{\cos\theta_r}{(\cos\theta_r + 1)}\left(h_o(\beta^- + 2c_o) - Q_i(\cos\theta_i - 1)\right) + O\left(\frac{Q_x}{c_o h_o}\right)^2 \tag{16}$$

It turns out, however, that for larger amplitude waves this expansion is one of the most significant error sources. It is therefore useful to carry the expansion of (15) to second order which yields a quadratic equation in $Q_{x,r}$. Again we can solve for $Q_{x,r}$ and eliminating the false root we then get the second order expression for $Q_{x,r}$:

$$Q_{x,r} = \frac{\cos\theta_r \left(c_o h_o(\cos\theta_r + 1) + Q_i(\cos\theta_i - \cos\theta_r - \frac{3}{2})\right)}{(2\cos\theta_r + \frac{3}{2})} \quad *$$

$$\left(\sqrt{1 - \frac{(4\cos\theta_r + 3)(Q_i^2(\frac{3}{4} - \cos\theta_i) + Q_i c_o h_o(\cos\theta_i - 1) - c_o h_o^2(\beta^- + 2c_o))}{(c_o h_o(\cos\theta_r + 1) + Q_i(\cos\theta_i - \cos\theta_r - \frac{3}{2}))^2}} - 1\right)$$
$$+O\left(\frac{Q_x}{c_o h_o}\right)^3 \tag{17}$$

These equations have two unknowns, $Q_{x,r}$ and θ_r, which can be determined by realizing that

$$\theta_r = \arctan\left(\frac{Q_{y,r}}{Q_{x,r}}\right) \tag{18}$$

The additional unknown $Q_{y,r}$ can be solved by using (9) which is rewritten as:

$$Q_{y,r} = \gamma\,(h_o + \bar{\zeta}) - Q_{y,i} \tag{19}$$

in which $Q_{y,i}$ is specified and γ is determined by integration of the last of the characteristic equations (7).

In these expressions β^- is the Riemann-variable updated to the next time level by (5). Q_i is the total flux of the known incoming wave at the same time level. From (16) or (17), and (18) and (19) we can find the unknowns $Q_{x,r}$ and θ_r iteratively. With the incoming wave known through specification, the boundary value of total flux Q_x can determined at the next time step.

4 Reflection properties

The absorption properties of the boundary condition are tested for a unidirectional wave in a domain of constant depth for various angles of incidence and wave amplitudes. In the following example waves are generated at the $x = 0$ and $y = 0$ boundaries and absorbed at all four boundaries for both versions of the boundary condition. The physical parameters are still water depth h_o and wave length $\lambda = 100\, h_0$, which yields a period $T = 100\sqrt{h_0/g}$. The numerical parameters are $\Delta x = \Delta y = \lambda/60$ and $\Delta t = T/100$ which yields a Courant number of 0.6. A second-order predictor-corrector numerical scheme is used for all tests.

Linear waves

In the first test, sinusoidal waves with a small amplitude $A/h_o = 0.01$ are propagated using the linear equations and absorbed using the boundary condition that applies the lowest order expansion of $Q_{x,r}$, (16). Sinusoidal waves are specified as the initial condition. This case was previously shown in Van Dongeren *et al.* (1994).

The reflection properties are computed for a square domain

$$\Omega_1 = \{(x, y) : 0 \leq x \leq \lambda, 0 \leq y \leq \lambda\} \tag{20}$$

where we want to make sure that the reflections are caused by one absorbing boundary (at $x = \lambda$) only. This is accomplished as follows. Solutions are computed in two domains: a rectangular domain

$$\Omega_2 = \{(x, y) : 0 \leq x \leq \lambda, 0 \leq y \leq 3\lambda\} \tag{21}$$

and in a larger, square domain,

$$\Omega_3 = \{(x, y) : 0 \leq x \leq 3\lambda, 0 \leq y \leq 3\lambda\} \tag{22}$$

see Fig. 4 for a definition sketch.

The non-generating boundaries in domain Ω_3 are placed so far away that they have no effect on the solution in the smaller domain Ω_1 during the duration of the simulation. Therefore in the smaller domain we can consider the Ω_3-solution free of reflection errors. Similarly, in domain Ω_2 the non-generating boundary at $y = 3\,\lambda$ will not influence the solution in the smaller domain Ω_1. Hence the difference between the two solutions can only be caused by the absorbing boundary at $x = \lambda$. The two solutions are subtracted from each other at the instant in time $t^n = T/\cos\theta_i$ when the initial condition has propagated out of Ω_1 and the difference is normalized by the amplitude A:

$$\epsilon_1(x, y, t^n; \theta_i) = \frac{|\,\bar{\zeta}_{\Omega_3}(x, y, t^n; \theta_i) - \bar{\zeta}_{\Omega_2}(x, y, t^n; \theta_i)\,|}{A} \tag{23}$$

where $\bar{\zeta}_{\Omega_2}$ and $\bar{\zeta}_{\Omega_3}$ are the solutions for the test runs in the domains Ω_2 and Ω_3, respectively.

Eq. (23) yields a spatial picture of the reflection error in Ω_1 due to the absorbing boundary condition at $x = \lambda$. Figs. 5a, c and e show contours of the spatial errors for three angles of incidence: $\theta_i = 0, \frac{\pi}{6}$ and $\frac{\pi}{4}$ where θ_i is defined as the angle between the direction of propagation and the x-axis. The errors are of the order 0.005 or 0.5%.

Note that the boundary condition is derived based on the nonlinear equations in characteristic form while the waves themselves are run under the linear equations, which is in itself inconsistent but allowable for small amplitude waves.

Nonlinear waves

To show the effect of the nonlinear terms in the equations, a second test is run for

the same parameters and for the same angles of incidence but using the nonlinear equations. The waves generated at the boundary are again sinusoidal. The spatial errors are plotted in Figs. 5b, d and f. Comparison to the previous case shows that including the nonlinear terms in the governing equations increases the error by a factor 2: they are now of the order of 1%. This is due to the fact that in the first order approximation (16), Eq. (14) reduces to the linear relationships of constant form

$$Q_{x,i} = c_o \bar{\zeta}_i \cos\theta_i \qquad Q_{x,r} = -c_o \bar{\zeta}_r \cos\theta_r \tag{24}$$

where c_o is given by (12). This means that the first order boundary condition absorbs constant form (linear) waves better than waves that change shape.

As can be seen in Fig. 5, the errors are spatially dependent. In order to obtain a single measure of the error as a function of the angle of incidence, the L^2-error is computed (Strikwerda, 1989). The L^2-error is defined as the squared difference of $\bar{\zeta}_{\Omega_2}$ and $\bar{\zeta}_{\Omega_3}$ evaluated in the domain Ω_1 and normalized by the RMS of the larger area solution at the time instant $t = t^n$ when the initial condition has propagated out (which is different for each θ_i):

$$\epsilon_2(t^n;\theta_i) = \frac{\sqrt{\sum_{\Omega_1}(\bar{\zeta}_{\Omega_2}(x,y,t^n;\theta_i) - \bar{\zeta}_{\Omega_3}(x,y,t^n;\theta_i))^2}}{\sqrt{\sum_{\Omega_1}(\bar{\zeta}_{\Omega_3}(x,y,t^n;\theta_i))^2}} \tag{25}$$

Figure 6 shows L^2-error for the range of angles of incidence of $\theta_i = [0, \frac{\pi}{12}, \frac{\pi}{6}, \ \ldots\ , \frac{\pi}{2}]$ for both the linear and nonlinear low-amplitude cases described above. Also plotted in Figure 6 is the error incurred when the Sommerfeld radiation condition (2) is applied for sinusoidal waves. This condition shows near-perfect absorption for waves of normal incidence but shows large errors for more obliquely incident waves. In fact, the error is 100% for glancing angles. In contrast, the errors due to the boundary

condition derived in Section 3 are of the order of 0.5% to 1% for the whole range of angles of incidence, which is acceptable for most applications.

However, the error is a function of the nonlinearity parameter, $\delta = A/h_o$. It can be shown that if (16) is applied in the boundary condition, the error $\epsilon_2 \sim \delta$. In a third test, the model is run for the same parameters as the previous test but with a wave with a ten times larger amplitude, $A/h_o = 0.1$. The spatial variation of the reflection errors, see Fig. 7a, c and e, are about one order of magnitude larger than in the previous test, as one should expect. Fig. 8 (dashed line) shows that the L^2-error versus θ_i for a single absorption boundary is about 10%, or $\delta * 100\%$, which is too large for practical purposes.

As mentioned in Section 3, a major error source for large amplitude waves is the first order expansion of (15). For larger amplitudes, it is therefore advantageous to use the second order approximation (17) as the boundary condition. The spatial errors as calculated by (23) are shown in Fig. 7b, d and f. We see that the error is now reduced by a factor 5 compared to the left-hand side panels. For a single absorbing boundary, the L^2-error versus the angle of incidence θ_i as calculated by (25) is shown in Fig. 8 (solid line). It has a magnitude of about 3%, which is close to the theoretical error $\epsilon_2 \sim \delta/4$ for the second order approximation. For our purposes, this magnitude of the error for medium height waves is acceptable.

Since the second order approximation (17) is explicit in $Q_{x,r}$, it does not require considerably more computational time than the linear expression (16) and it will therefore be used in the remainder of this paper.

5 Example of simultaneous absorption and generation

To illustrate the application of the proposed boundary condition for the case of simultaneous absorption and generation of waves at one boundary, consider a domain with an absorbing-generating boundary at the $x = 0$ boundary and a wall at $x = 4.25\lambda$. From a cold start, incoming waves are generated at normal incidence from $t = 0\,T - 19\,T$, tapered with a hyperbolic tangent function during the first and last period of generation in order to eliminate transients due to shocks. This wave train will reflect off the wall at $x = 4.25\lambda$ and produce a standing wave until the incident waves are turned off at $T = 19T$. Parameters used are: water depth h_o, wave length $\lambda = 100h_o$, $T = \lambda / \sqrt{g\,h_o}$, $A = 0.01h_o$, $\Delta x = \Delta y = \frac{\lambda}{60}$ and $C_r = 0.6$. The numerical scheme for the linearized equations is used in this example.

Fig. 9a shows the time series of the specified volume flux of the incident waves at $x = 0$, normalized by $c_o\,h_o$. The effect of the hyperbolic tangent function is clearly visible as the amplitude grows to its full value in little more than one wave period. Fig. 9b shows the flux of the outgoing wave train at the same point as calculated by (17). The outgoing wave train is a near-perfect mirror image of the incident wave train except for some small trailing waves around $t = 28\,T$. Still water is recovered almost immediately after the outgoing wave passes through the $x = 0$ boundary, which indicates that the reflections are small. The time series of the total flux in Fig. 9c, which is the sum of the two time series above, shows first a progressive wave in the $+x$ direction, then the anti-node of the flux of a standing wave, then a progressive wave in the $-x$ direction and finally still water. This Figure qualitatively shows that the absorbing-generating boundary condition works very well.

In order to measure the reflection error due to the absorbing-generating boundary condition, the envelope of the standing wave, $\hat{\zeta}$, is calculated when the front of the incident wave train has propagated through the domain and has almost reached the $x = 0$ boundary (which happens at $t = 8.5\,T$). The envelope is shown in Fig. 10a (solid line). This Figure does not show the entire domain because the tapered front of the wave does not produce a standing wave at this time. The standing wave is a result of the summation of the incident wave train and its reflection off the wall and has a maximum amplitude of $2\,A$. When the front of the wave train reaches the open boundary at $t = 8.5\,T$, it will be absorbed almost perfectly as indicated in Fig. 9b. However, a small portion of the wave with amplitude A_ϵ will be reflected and propagate back in the $+x$ direction. This small error wave will itself reflect from the back wall and produce a standing wave of its own. Again, the envelope of the total standing wave (the standing wave due to the specified wave and the error wave) can be calculated at a time just before this small error wave reaches the open boundary, which happens at $t = 17\,T$. This envelope, $\hat{\zeta} + \hat{\zeta}_\epsilon$, has a maximum amplitude of $2(A + A_\epsilon)$ and is shown as the dashed line in Fig. 10a. Due to the smallness of the error wave, the dashed line is almost indistinguisable from the solid line. A measure of the error in amplitude caused by the generating-absorbing boundary can then be defined as the difference between the two envelopes normalized by the amplitude of the original standing wave or

$$\epsilon_3 = \frac{\hat{\zeta}_\epsilon}{2\,A} \tag{26}$$

which is shown in Fig. 10b and has a maximum of about 0.2%.

6 Discussion

The numerical tests described above show that the reflection errors due to the present boundary condition are of the order of only a few percent for cases of absorption-generation as well as absorption only. This is a remarkable improvement over the absorption properties of the widely-used radiation conditions based on the wave equation, which only absorb waves at one specific angle of incidence perfectly and show large errors for other angles of incidence.

In its present form the boundary condition has one major drawback. It cannot absorb multiple waves with a difference between angles of incidence larger than $\frac{\pi}{2}$. This is due to the fact that by using (14) the set of multiple waves at the boundary is essentially approximated by one representative progressive wave which is not valid when two or more wave trains intersect at oblique angles.

It is emphasized that for simplicity the present form of the boundary condition does not account for time-varying or steady currents. However, the mathematical modification of either (16) or (17) to include currents is straightforward. The real problem, as stated in Section 2, lies in the philosophical distinction between currents and long waves and in the fact that currents would have to be known à priori and specified along all boundaries of the domain.

7 Conclusions

In this paper two orders of an absorbing-generation boundary condition for the nonlinear shallow water equations are derived based on the Method of Characteristics. Numerical tests show that by using this boundary condition, reflection errors

can be limited to a few percent of the incident wave amplitude for the full range of angles of incidence, which is an improvement over the classical radiation conditions. Unlike those radiation conditions, the present boundary condition allows simultaneous specification of an incident wave train and absorption of an outgoing wave train at the same boundary, which makes it particularly suitable for application on artificial oceanside boundaries in shallow water models.

Acknowledgments

This work is a result of research sponsored by NOAA Office of Sea Grant, Department of Commerce, under Award No. NA 56 RG 0147 (Project No. R/OE-17) and by the U.S. Army Research Office, University Research Initiative under Contract No. DAAL03-92-G-0016. The U.S. Government is authorized to produce and distribute reprints for government purposes notwithstanding any copyright notation that may appear herein.

Appendix I. References

Abbott, M.B. (1979). Computational Hydraulics. Elements of the Theory of Free Surface Flow. Pitman Publishing, 324 p.

Broeze, J. and E.F.G. Van Daalen (1992). Radiation boundary conditions for the two-dimensional wave equation from a variational principle. *Math. Comp., vol. 58, no. 197*, pp. 73-82.

Engquist, B. and A. Majda (1977). Absorbing boundary conditions for the numerical simulation of waves. *Math. Comp., vol. 31, no. 139*, pp. 629-651.

Givoli, D. (1991). Non-reflective boundary conditions. *J. of Comp. Physics, vol. 94*, pp. 1-29.

Hibberd, S. (1977). Surf and run-up. Ph.D. dissertation, School of Mathematics, University of Bristol, 124 p.

Higdon, R.L. (1986). Absorbing boundary conditions for difference approximations to the multi-dimensional wave equation. *Math. Comp., vol. 47, no. 176*, pp. 437-459.

Higdon, R.L. (1987). Numerical absorbing boundary conditions for the wave equation. *Math. Comp., vol. 49, no. 179*, pp. 65-90.

Keys, R.G. (1985). Absorbing boundary conditions for acoustic media. *Geophysics, vol. 50, no. 6*, pp. 892-902.

Kobayashi, N., A.K. Otta and I. Roy (1987). Wave reflection and run-up on rough slopes. *Journal of Waterway, Port, Coastal and Ocean Engineering, ASCE, vol. 113, no. 3*, pp. 282-298.

Sommerfeld, A. (1964). Lectures on Theoretical Physics. Academic Press, New York.

Strikwerda, J.C. (1989). Finite difference schemes and partial differential equations. Wadsworth & Brooks/Cole Mathematical Series. Wadsworth, Belmont, California, 386 pp.

Svendsen, I.A. (1974). Cnoidal waves over a gently sloping bottom. *Series paper # 6*, Institute of Hydrodynamics and Hydraulic Engineering, Technical University of Denmark, 181 pp.

Svendsen, I.A. and P. Justesen (1984). Forces on slender cylinders from very high waves and spilling breakers. *Symposium on description and modelling of directional seas.* Copenhagen 1984. Chapter D-7, 16 pp.

Svendsen, I.A. and U. Putrevu (1995). Surf-zone hydrodynamics. *Research report CACR-95-02*, University of Delaware, 71 pp.

Van Dongeren, A.R., F.E. Sancho, I.A. Svendsen and U. Putrevu (1994). SHORECIRC: A quasi 3-D nearshore model. *Proc. of the 24th ICCE*, pp. 2741-2754.

Van Dongeren, A.R., I.A. Svendsen and F.E. Sancho (1995). Application of the Q-3D SHORECIRC model to surfbeat. *Proc. Coastal Dynamics*, pp. 233-244.

Verboom, G.K., G.S. Stelling and M.J. Officier (1981). Boundary conditions for the shallow water equations. *In:* Abbott, M.B. and J.A. Cung *Eds.*, *Engineering Applications of Computational Hydraulics*, vol. I, pp. 230-262.

Verboom, G.K and A. Slob (1984). Weakly-reflective boundary conditions for two-dimensional shallow water flow problems. *Adv. Water Resources, vol. 7*, pp. 192-197.

Whitham, G.B. (1974). Linear and nonlinear waves. John Wiley and Sons, New York, 636 pp.

Appendix II. Notation

The following symbols are used in this paper:

A	-	wave amplitude
A_ϵ	-	amplitude of reflected wave
c	-	nonlinear shallow water phase speed
c_o	-	linear shallow water phase speed
f_x, f_y	-	forcing terms in NSW-equations
$F_{\beta+}, F_{\beta-}, F_\gamma$	-	forcing terms in Equations in Characteristic Form
g	-	gravity
h	-	total water depth
h_o	-	still water depth
P	-	eigenvector space
Q	-	total flux
Q_x, Q_y	-	total flux in x and y directions
Q_i	-	total flux of the incoming wave
$Q_{x,i}, Q_{y,i}$	-	flux of the incoming wave in x and y directions
$Q_{x,r}, Q_{y,r}$	-	flux of the outgoing wave in x and y directions
$\bar{Q}$	-	total flux of the current
$\bar{u}, \bar{v}$	-	shortwave averaged and depth averaged horizontal velocities
T	-	wave period
β^+, β^-, γ	-	Riemann variables
δ	-	nonlinearity parameter
$\epsilon_1, \epsilon_2, \epsilon_3$	-	reflection errors
$\bar{\zeta}$	-	shortwave averaged surface elevation
$\bar{\zeta}_i, \bar{\zeta}_r$	-	surface elevation of incoming and outgoing wave
$\bar{\zeta}_{\Omega_2}, \bar{\zeta}_{\Omega_3}$	-	surface elevation computed in the domains Ω_2 and Ω_3
$\bar{\bar{\zeta}}$	-	infragravity wave-averaged surface elevation
$\hat{\zeta}, \hat{\zeta}_\epsilon$	-	envelopes of the standing wave
λ	-	wave length
θ_n	-	angle of incidence of the radiated waves
θ_i, θ_r	-	angle of incidence of incoming and outgoing wave
ϑ	-	angle between boundary and x-coordinate axis
$\Omega_1, \Omega_2, \Omega_3$	-	domains used in reflection tests

Keywords

absorbing boundary conditions

absorbing-generating boundary conditions

boundary conditions

method of characteristics

nonlinear shallow water equations

numerical applications

numerical modelling

numerical reflections

shallow water models

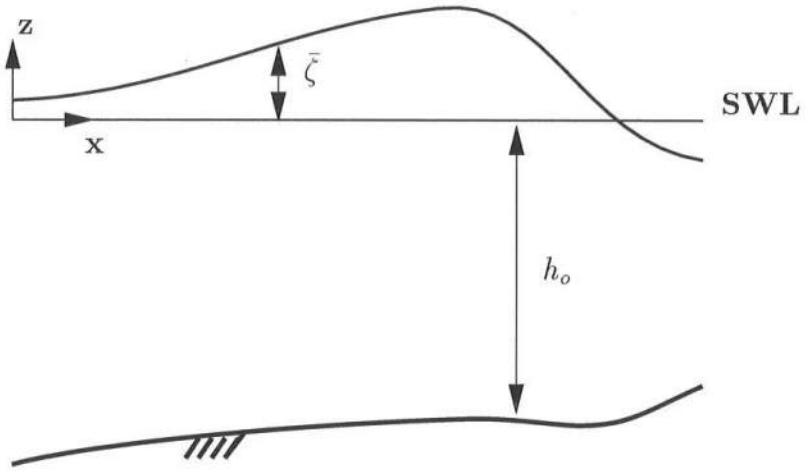

Figure 1: Definition sketch.

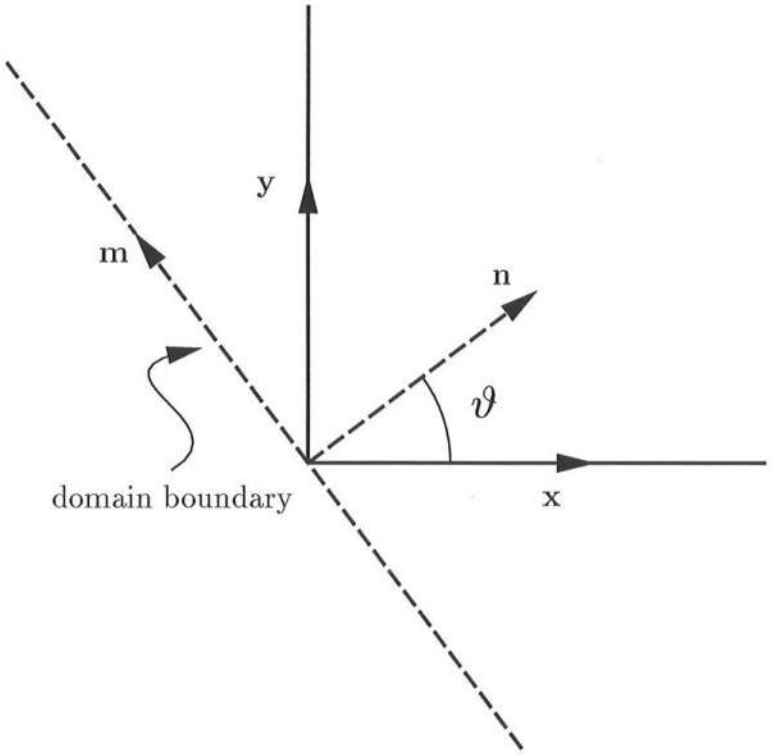

Figure 2: Coordinate system.

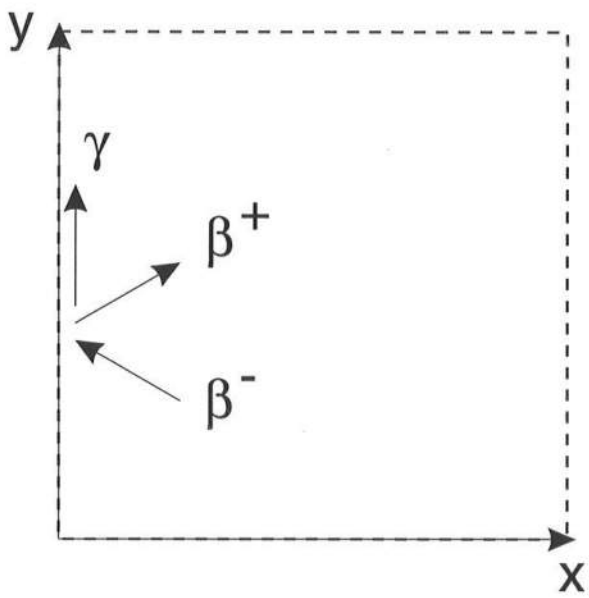

Figure 3: Definition sketch of the characteristics.

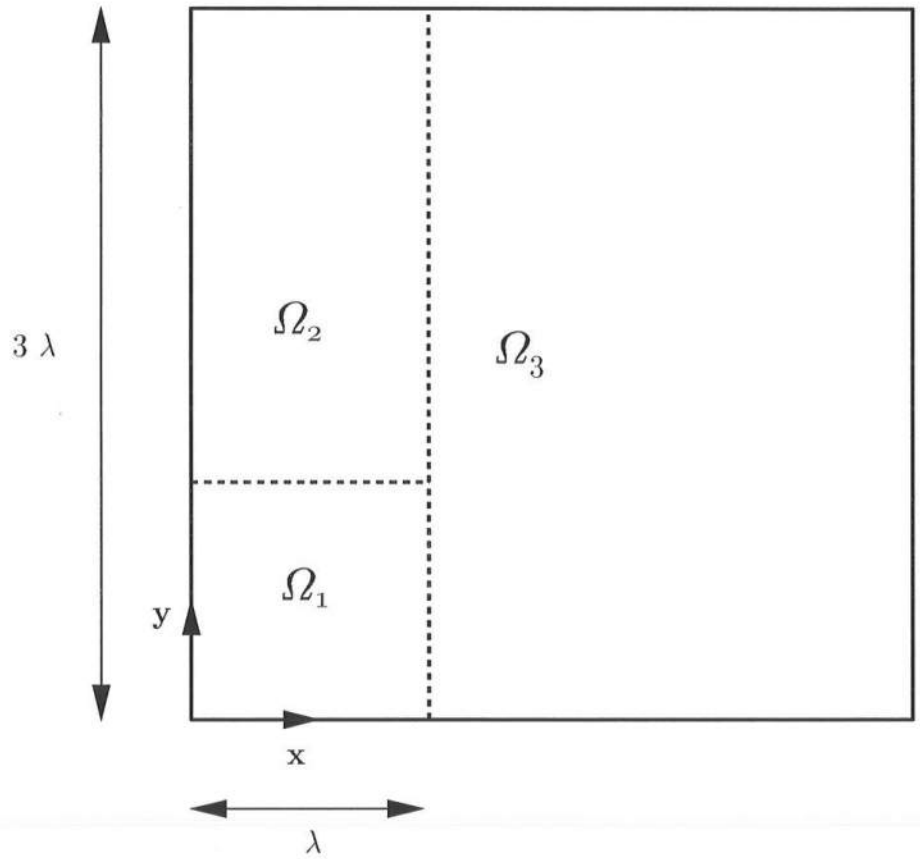

Figure 4: Definition sketch of the domains used in the reflection tests.

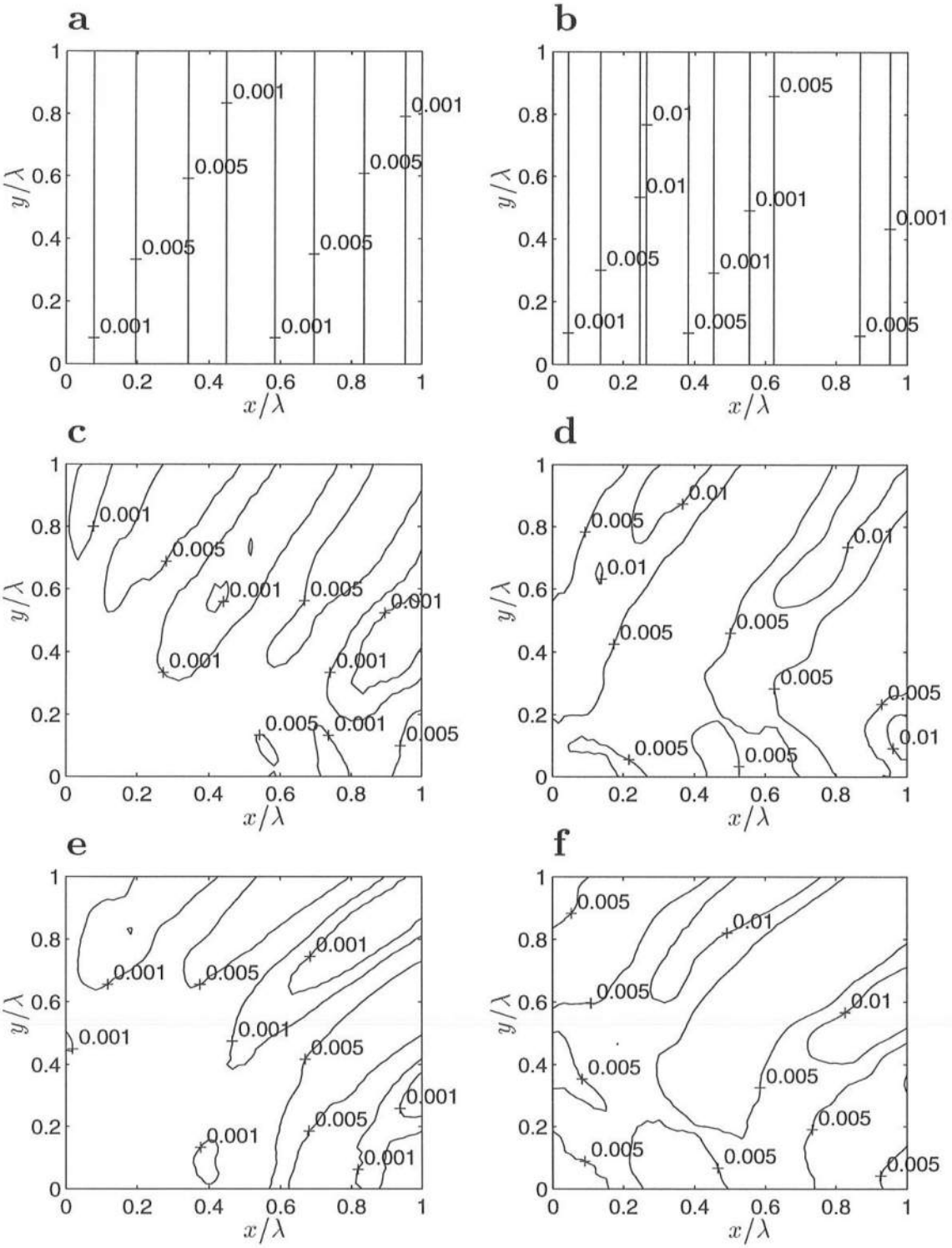

Figure 5: Reflection errors vs $(x/\lambda, y/\lambda)$ for wave amplitude $\mathrm{A}/h_o = 0.01$ using (16) (a) linear scheme, $\theta_i = 0$, at $t^n = T$; (b) nonlinear scheme, $\theta_i = 0$, at $t^n = T$; (c) linear scheme, $\theta_i = \frac{\pi}{6}$, at $t^n = T/\cos\frac{\pi}{6}$; (d) nonlinear scheme, $\theta_i = \frac{\pi}{6}$, at $t^n = T/\cos\frac{\pi}{6}$; (e) linear scheme, $\theta_i = \frac{\pi}{4}$, at $t^n = T/\cos\frac{\pi}{4}$; (f) nonlinear scheme, $\theta_i = \frac{\pi}{4}$, at $t^n = T/\cos\frac{\pi}{4}$.

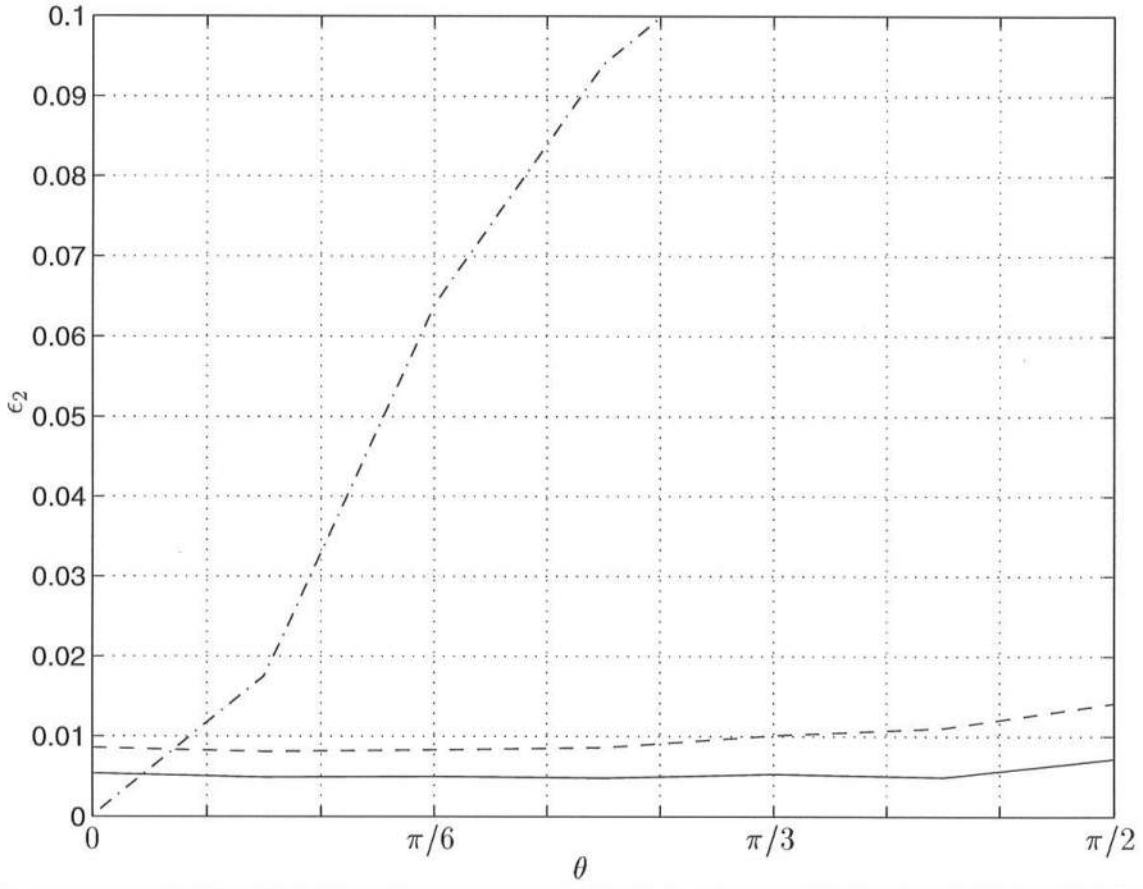

Figure 6: Reflection error vs. angle of incidence θ_i for $A/h_o = 0.01$. First order BC: linear scheme (solid line), nonlinear scheme (dashed line). Sommerfeld radiation condition: linear scheme. (dash-dot line)

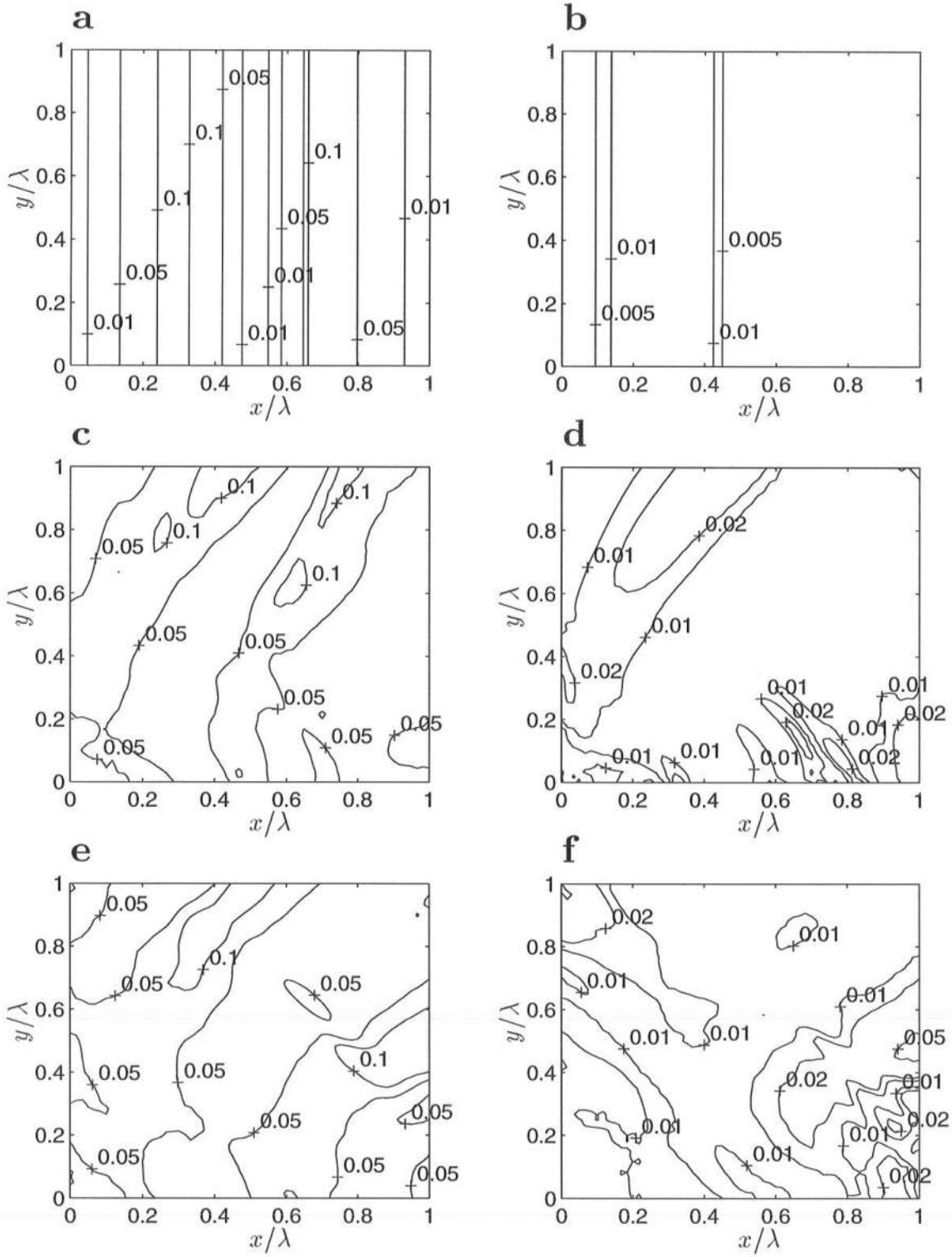

Figure 7: Reflection errors vs $(x/\lambda, y/\lambda)$ for wave amplitude $A/h_o = 0.1$ and a nonlinear scheme (*a*) $\theta_i = 0$, at $t^n = T$, first order BC; (*b*) $\theta_i = 0$, at $t^n = T$, second order BC; (*c*) $\theta_i = \frac{\pi}{6}$, at $t^n = T/\cos\frac{\pi}{6}$, first order BC; (*d*) $\theta_i = \frac{\pi}{6}$, at $t^n = T/\cos\frac{\pi}{6}$, second order BC; (*e*) $\theta_i = \frac{\pi}{4}$, at $t^n = T/\cos\frac{\pi}{4}$, first order BC; (*f*) $\theta_i = \frac{\pi}{4}$, at $t^n = T/\cos\frac{\pi}{4}$, second order BC.

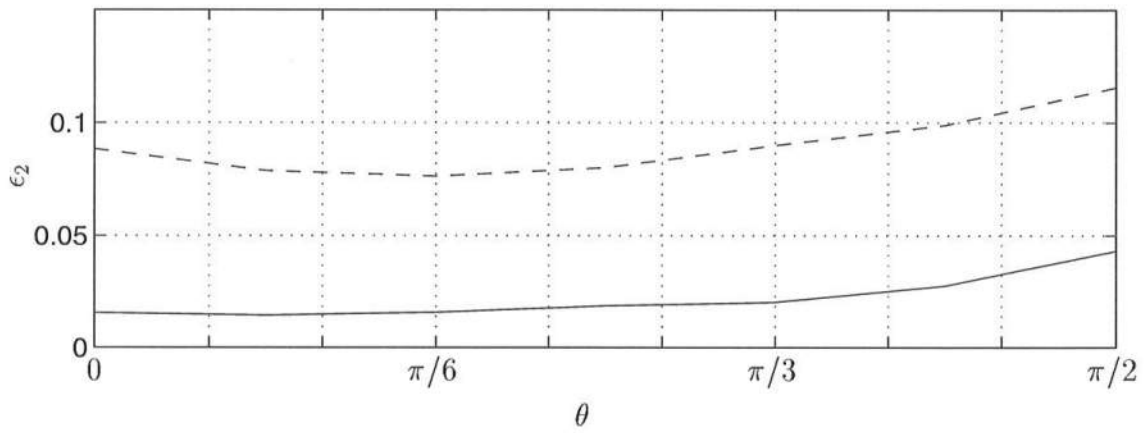

Figure 8: Reflection error vs. angle of incidence θ_i for $A/h_o = 0.1$. First order BC (dashed line), second order BC (solid line).

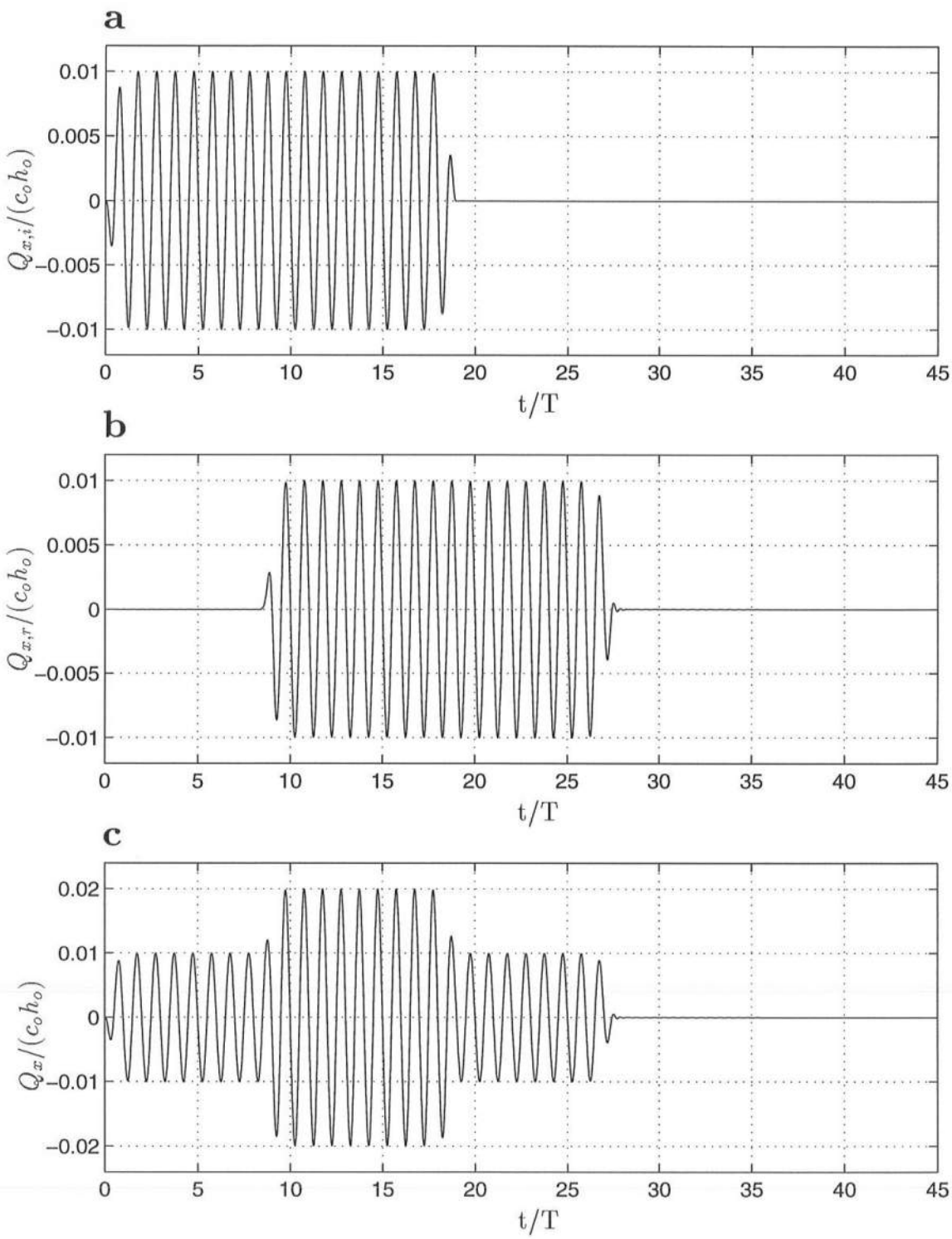

Figure 9: Time series at $x = 0$: (a) incident wave flux. (b) outgoing wave flux. (c) total flux.

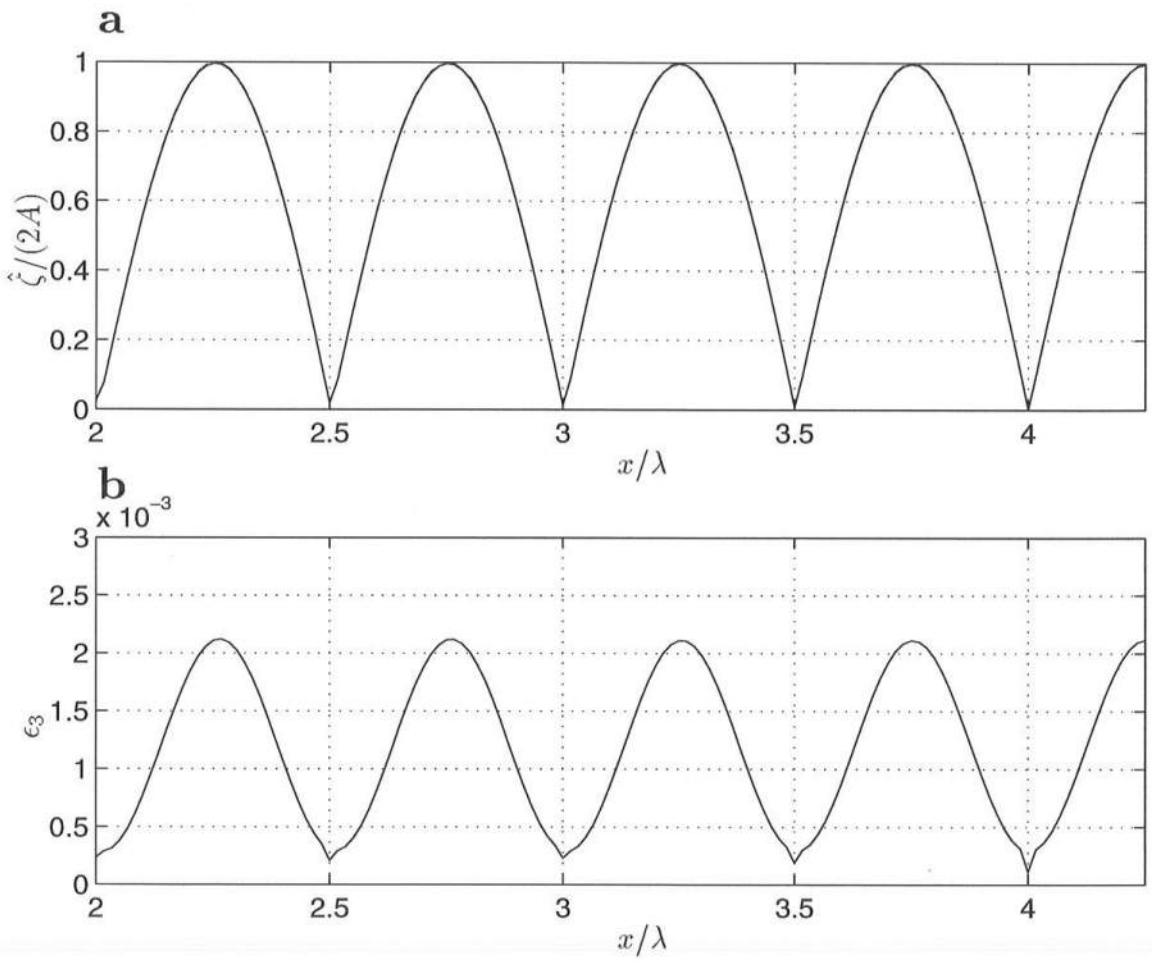

Figure 10: (*a*) Envelope of the standing wave of the incident wave (solid line) and of the incident and error wave (dashed line). (*b*) Normalized difference between the two envelopes.